J Nanostruct 14(4): 1029-1039, Autumn 2024

RESEARCH PAPER

Effect of Gold Nanoparticles on *hmgA* Gene Expression of Pseudomonas aeruginosa Isolates

Iman Abbas AL-Essawi [1]***, and Huda M. Mahmood*** [2*]

[1] *Fallujah Teaching Hospital, Microbiology Laboratory, Fallujah, Al-Anbar, Iraq*

[2] *College of Science, Department of Biotechnology, University of Anbar, Ramadi, Al-Anbar, Iraq*

ARTICLE INFO

Article History:
Received 03 July 2024
Accepted 25 September 2024
Published 01 October 2024

Keywords:
Gold NPs
hmgA gene
Pseudomonas aeruginosa
Pyomelanin pigment

ABSTRACT

The present study was designed to explore the effect of gold nanoparticles on the *hmgA* gene expression and pyomelanin pigment production from local *Pseudomonas aeruginosa* isolates. Out of 162 patients suffering from ear infections, urinary tract infections, burns, wounds, cerebrospinal fluid (CSF), respiratory tract infections (RTI), and blood infection (sepsis), eight isolates identified to produce pyomelanin pigment (8.42%). All isolates were characterized using microscopical, morphological, and biochemical methods, VITEK-2 compact systems, and 16SrRNA gene, which showed that all these isolates belong to *P. aeruginosa*. Screening producing pyomelanin pigment was carried out by using a specific media to promote the production of pyomelanin pigment. The extracted pyomelanin pigment was purified using simple acid sedimentation followed by centrifugation to extract the crude product and purify it with HPLC. The purified pigment was positive for all major physical and chemical tests that characterize pyomelanin pigment, including UV-visible spectroscopy and Fourier transform infrared spectroscopy (FT-IR). The study also covered the preparation of gold nanoparticles using the green chemistry method, which used black tea-leaf extract. The resulting nanoparticles were positive for all significant qualitative tests used to characterize them, including UV-visible spectroscopy (FT-IR), X-ray diffraction (XRD), and SEM. The results of the SEM image showed spherical particles with a size of approximately 19nm nanoparticles. In conclusion, the effect of the prepared gold nanoparticles on the gene expression of the *hmgA* gene was studied at different concentrations compared to the control sample using a real-time one-step polymerization reaction, also the gene expression results showed that the gold nanoparticles significantly increased the gene expression of the *hmgA* gene.

How to cite this article
AL-Essawi I., Mahmood H. Effect of Gold Nanoparticles on hmgA Gene Expression of Pseudomonas aeruginosa Isolates. J Nanostruct, 2024; 14(4):1029-1039. DOI: 10.22052/JNS.2024.04.004

INTRODUCTION

Pseudomonas aeruginosa is an opportunistic Gram-negative rod bacterium that lives in all wet and dry environments and animal tissues [1]. It is also one of the primary pathogens, especially in patients with urinary tract infections, burns, cystic fibrosis, and bacteremia. It possesses a natural resistance to many antibiotics, which causes widespread deaths in immunocompromised patients [2]. *P. aeruginosa* is an occasional pathogen

* *Corresponding Author Email: huda.mahmood@uoanbar.edu.iq*

able to invade nearly all tissues. Furthermore, *P. aeruginosa* is a germ widely distributed worldwide [3]. *P. aeruginosa* produces several extracellular pigments that are important for virulence factors associated with its pathogenicity and virulence; among them are pyocyanin and pyomelanin pigments [4,5]. Pyocyanin blue phenazine belongs to the phenazine group, a redox-action pigment. It is considered an antibiotic for several microorganisms [6,7, 60]. Pyomelanin pigment is an extracellular brown pigment with high molecular weight and negative charge from the tyrosine catabolism pathway [8]. Several studies reported that pyomelanin pigment is produced from *P. aeruginosa*, isolated from the urinary tract and cystic fibrosis infections [9]. As a means of protection from light and free radicals for survival, it is also involved in iron reduction and acquisition and extracellular electron transport [10].

Gold NPs have long been used due to their unique optical, photochemical, and electronic properties[11]. The Chinese used colloidal red gold as medicine, which was used in Indian medicine [12]. The gold NPs are used in cosmetics and hair tonics[13]. Gold NPs emerged as an effective gene carrier due to their large surface area, low cell toxicity, and stability[14]. Also, it can escape from the lysosome digestions, protecting the DNA or the genes that carry it from degradation [15]. The gold nanoparticles produced by the bacteria showed no toxic effect on *P. aeruginosa* [16]. It inhibits biofilm formation [17]. Gold NPs interfere with bacterial cellular communication systems and influence the expression of many virulence factors [18]. This study aimed to use prepared gold NPs by green chemistry method using black tea leaf extract and investigate their effect on the hmgA gene expression involved in the biosynthesis of pyomelanin pigment.

MATERIALS AND METHODS

One hundred and sixty-two samples were obtained from different sources (ear, burns, sputum, blood, and urine) and collected from patients from other hospitals in Al-Anbar. The collected samples were inoculated on MacConkey agar at 37˚C for 48 h. to select pale colonies, then subcultured on Cetrimide agar to obtain pure colonies. These isolates were diagnosed by morphological and biochemical tests and re-confirmed by VITECK-2 and *16Sr RNA.* All *P. aeruginosa* isolates were cultured on tyrosine production medium to obtain pyomelanogenic isolates and incubated at 37°C for 48h, then incubated at room temperature for six days. Mutants producing a brown pigment after incubation, referring to the positive result of pyomelanin production, were selected [19, 20, 60].

Pyomelanin pigment was extracted from the culture of the pyomelanin production medium. Isolation and purification were carried out according to the reported method described by Singh[21]. HPLC analyzed samples using Shimadzu LC-2010 AHT liquid chromatography (Japan) with Reodyne 7125, 20µl injector. Shimdzu SPD-2010 A UV-visible detector set at 272 nm and the column used (250×4.6mm) C18, and a 5 µm particle size was used at room temperature. Concentrations of L-tyrosine HGA and pyomelanin were determined by calculations of peak areas at 272 nm and comparisons with standard agents of L-tyrosine, HGA, and pyomelanin [22]. Purified pyomelanin pigment was prepared using the initial concentrations of 100 mg in 3 ml of 0.1 N HCL. The solution was scanned from 190 to 1100 nm wavelengths using Shimadzu Spectrophotometer, and 0.1N HCL was used as the blank[23]. The spectroscopic properties of the pheomelanin pigment obtained from pyomelanogenic *P. aeruginosa* isolates were compared with those of the standard synthetic pheomelanin pigment obtained from Mahmood et al. [24].

Using KBr disks with an FTIR spectrophotometer (FT/IR-4100; Shimadzu-Japan) at 4000-400 cm-1, the purified lyophilized pigment was used for FTIR analysis. Peak max changes were analyzed in various spectrum regions [25].

Preparation of gold nanoparticles (AuNPs)

The gold nanoparticles were prepared according to Sharma [26] as follows:

One gram of $HAuCl_4$ (99% Germany) was dissolved in 200 ml distilled water in a 500 ml flask to obtain a solution of $HAuCl_4$ (12 mM), which was stored in a brown bottle. The tea extract was prepared using 0.34 gm of black tea leaves in 100 ml of distilled water. It was heated on a magnetic heating pad for 15 minutes at 70-80°C and then filtered with Whatman filter paper No.1.

Synthetic AuNPs were synthesized by reducing $HAuCl_4$ to Au**.** A 100 ml of $HAuCl_4$ solution (12 mM) was mixed with black tea leaf extract (100 ml) on a magnetic stirrer hotplate at 80°C; the color of the mixture turned purple within 10-15min,

indicating the production of gold nanoparticles, then sterilized the solution using a filter syringe 0.22µm. The AuNPs were then harvested by centrifugation at 12000 rpm for 20 min, washed three times with sterile distilled water, and dried at 40°C for 48 hours [27,28].

Characterization of AuNPs

AuNPs were characterized by V-visible, SEM, FTIR, and XRD to identify their chemical and physical properties.

UV-visible Spectroscopy

Analysis was performed to identify the absorbance of the visible and UV light spectrum at 400-600 nm wavelengths to monitor the interaction between gold ions and tea extract [26]. The gold NPs solution was diluted with sterile distilled water in a ratio of 1:9 ml using distilled water as a blank.

Infrared Spectroscopy measurements

FTIR analysis to identify functional groups of nanoparticles after they were deposited on a glass slide to dry. Then, they mixed with potassium bromide (KBr) granules in a ratio of 1: 100 until they were in a disc form. Then were measured with (an FTIR-4100; Shimadzu-Japan) spectrophotometer[29].

X-ray diffraction pattern

The structural characterization of the manufactured gold nanoparticles was analyzed as the sample was placed in powder form on a glass slide [30]. X-ray diffraction device operating at a wavelength of 1.54060 with a Step Size of [°2Th] 0.0500.

Scanning Electron Microscopy (SEM)

Scanning Electron Microscopy (SEM) was used to determine the morphological structure of the

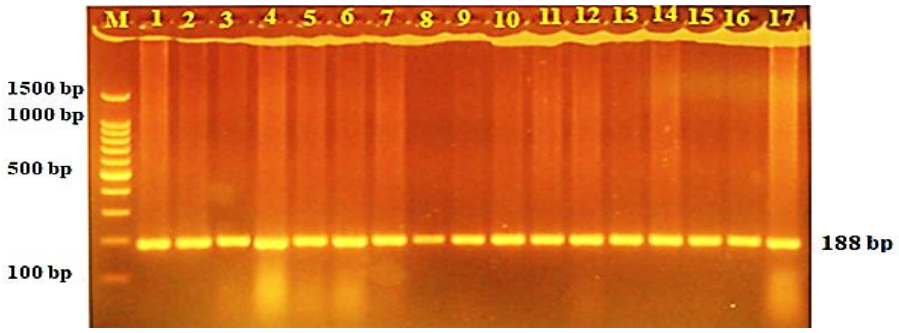

Fig. 1. Amplification of *16SrRNA* gene of *Pseudomonas aeruginosa* samples were fractionated on 1% agarose gel electrophoresis stained with ethidium bromide. M: 100bp ladder marker. Lanes 1-17 resemble 188bp PCR products.

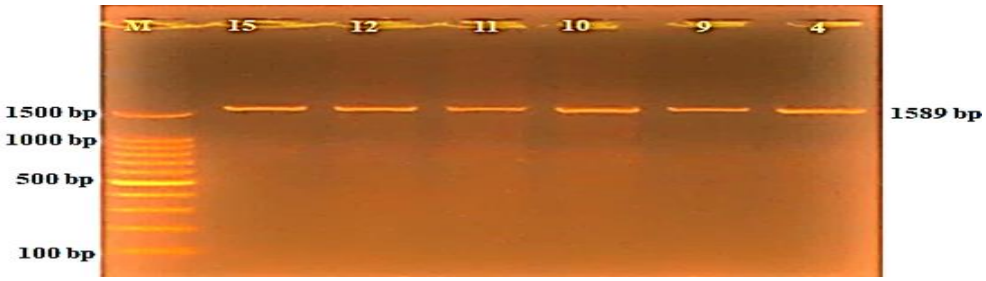

Fig. 2. Amplification of *hmgA* gene of *Pseudomonas aeruginosa* isolates were fractionated on 1% agarose gel electrophoresis stained with ethidium bromide M: 100bp ladder marker. Lanes 4, 9, 10, 11, 12, and 15 resemble 1589bp PCR products.

surface layer [31]. The analysis involves scanning the sample and focusing the electron beam accurately to obtain microscopic images of the surface of the prepared gold nanoparticles [32].

Preparation of pigment-producing P. aeruginosa isolates

By mixing 0.1gm of AuNPs with 10 ml of distilled water (10 mg/ml), the stock solution of gold nanoparticles was prepared in concentrations (10, 20, 40, 80, 160, 320, and 10000µg /ml) by mixing the known amount of the stock solution with sterile distilled water. The bacteria suspension was prepared and compared with McFarland No. 0.5, then 100 µl of bacterial suspension were transferred to Luria broth, and tyrosine broth inoculated with 100µl of AuNPs concentrations (0, 10, 20, 40, 80, 160, 320, and 10000µg / ml) then incubation of tubes at 37 for 18-24 hrs. [26, 33]. RNA was extracted from these replicates. The real-time one-step technique was used to quantify the gene expression level of *phzM* and *hmgA* genes compared to the *oprl* gene (reference gene).

RESULTS AND DISCUSSION

Out of one hundred sixty-two specimens of ear infection, urinary tract infection (UTI), burns, wounds, respiratory tract infection (RTI), blood, and cerebrospinal fluid (CSF), ninety-five isolates of *P. aeruginosa* were obtained from the total number of study specimens with an isolates rate of 58.6% which was characterized by its growth on Cetrimide agar media (0.3%). Molecular identification of *Pseudomonas aeruginosa* was carried out using the *16SrRNA* gene sequence (Fig. 1). Pyomelanin pigment was produced after 3-4 days and cultured on pyomelanin pigment production media. The percentage of isolates producing pyomelanin pigment was 62.5 % from the ear, 12.5 % from UTI, and 25 % from the blood.

Six isolates carried the *hmgA* gene responsible for producing the pyomelanin pigment using the polymerase chain reaction (PCR). The PCR products of the *hmgA* gene (1589bp) were confirmed using a gel electrophoresis system (Fig. 2). This result was in agreement with Rodríguez-Rojas *et al* study, which was found that *P. aeruginosa* isolates produced the pyomelanin pigment contained the mutant *hmgA* gene [34]; also, it comes in agreement with Mahmood *et al* [24].

Extraction and purification of pyomelanin pigment

Studying bacterial pigments requires separating and purifying the pigment from the biological environment in which it is found. It is a method used to preserve pigment during isolation and obtain it in its original form. The extraction method used for pyomelanin is inexpensive and easy to apply in two steps; the pigment was precipitated by acid (1N) HCl pH 2, followed by a centrifuge of the pigment, which precipitates as brown sediment. The pyomelanin purification method was identical to the protocol used in previous studies [35, 36]. The purified pyomelanin pigment gave a positive result in the primary tests used to characterize the pigment.

Spectral characterization of purified pyomelanin pigment

To better characterize the pyomelanin pigment, it is helpful to understand its structure, although until recently, the characterization of pyomelanin was elusive due to its size and complexity. The

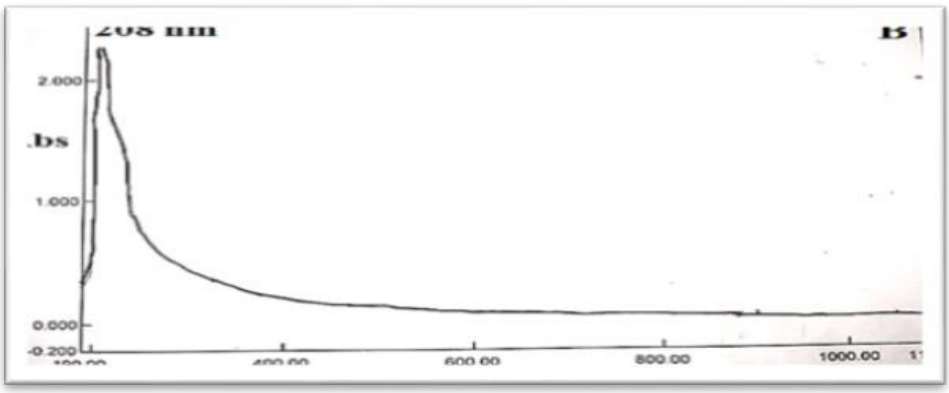

Fig. 3. UV absorbance for purified pyomelanin pigment.

relative purity of HGA-melanin gave an excellent start to determining the structure of bacterial pyomelanin, even though most microbial pigments contain metabolism residues [37]. UV and FTIR techniques were used to characterize pyomelanin in this study samples.

UV-VIS Spectrophotometry characterization

The spectral properties of the pyomelanin pigment were detected using the ultraviolet spectrum on the samples, where the maximum UV absorption peaks were in the range of 208-300 nm, and for standard pyomelanin 235-300 nm as shown in (Fig. 3) this typical for brown pigment. A gradual decrease in absorbance offsets the increase in wavelength in the UV region. This is the most crucial feature of the pyomelanin pigment [38]. In other words, the relationship between the optical density and wavelength of the pyomelanin solution in the graph showed a negative slope with a linear curve. The reason that all of the absorption spectra were strong at the range of 200-300 nm could be due to the complex structures conjugated to the molecule of pyomelanin pigment. The presence of oxygen-containing systems also contributed to the dark color of the pyomelanin pigment. Therefore, the pyomelanin pigment has efficiently converted the absorbed photon energy from ultraviolet rays to heat, and the speed of this process reduces harmful damage to optical chemicals. Therefore, it can be said that pyomelanin pigment protects microorganisms from harmful radiation. Melanin pigment can dissipate more than 99% of UV rays into harmless heat, indirectly preventing DNA damage, which is usually the cause of skin cancers [39].

Fourier transform infrared spectroscopy

Fourier transform infrared spectroscopy **(**FTIR) is one of the most accurate methods in analyzing and identifying the structure of melanin and its functional groups. This technique gives high-resolution spectral data using a broad spectrum of infrared rays [40]. FTIR results of (HGA-melanin) absorbance peaks were compatible with the polymeric structures of OH stretch, aliphatic- C-H bonds, aromatic C=C bonds associated with C=O and/or COO groups, and phenolic OH group is revealed [41, 42].

The purified pyomelanin was tested with FTIR for characterization and results compared with other results of the standard pyomelanin (Fig. 4). The pigment absorption results for infrared spectra showed several peaks representing their functional groups, where a broad peak appeared at 3448 cm^{-1}, which belongs to the linked or polymeric hydroxyl group. The peak at 2924 cm^{-1} indicates the aliphatic groups, which are the hydrogen hydroxide group and the presence of an aldehyde –CH bond group. Area analysis of 1500-2000 cm^{-1} shows well-defined maxima at 1720, 1628cm^{-1} and 1544 cm^{-1}; these maximal absorption peaks were allocated to carbonyl C=O and aromatic rings, C=C/C=N double bonds and conjugated with C=O and/or COO groups. Although 1460 cm^{-1} corresponded to the modes of C-H vibration, 1372 cm^{-1} corresponded to the modes of oscillation of O-H alcohol groups. The binding of metal ions to the HMG-melanin pigment caused

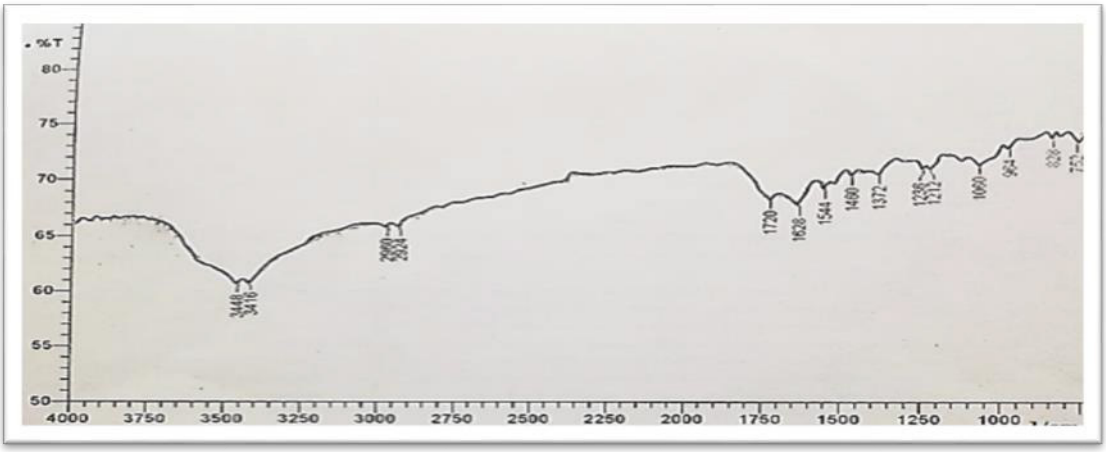

Fig. 4. FTIR analysis of purified pyomelanin pigment.

a change in the FTIR vibration that was affected by the adsorption ratio. The 1060 cm^{-1} and 752 cm^{-1} peaks are associated with the asymmetric stretching vibrations of the -C-N and -C-H aromatic groups, respectively. These results showed a high degree of similarity with the absorbance peaks of the standard pyomelanin [22].

Biosynthesis of gold nanoparticles by green chemistry method

An eco-friendly method was used to prepare gold nanoparticles, where dry black tea leaves that contain polyphenols, which is a good reducing agent for the formation of NPs and phytochemicals, which include water-soluble catechins that act as a reducing agent and envelop the surface of the gold particles to prevent their clumping [43, 44]. Water has also been used as an environmentally harmless solvent [26]. The preparation was done by using a stock solution of gold chloride with a stock solution of tea leaves mixed at 60°C for 15 min, where the solution turned into a deep purple color, indicating the formation of gold nanoparticles (AuNPs) (Fig. 5), the color change is a sign of interaction between tea extract and gold chloride tetrahydrate ($HAucl_4$), this color change is due to the excitation of the Plasmon surface as a result of the collective movement of free electrons present in the nanoparticles in the visible light area[45].

Characterization of gold nanoparticles (AuNPs) UV-visible analysis

The visible and ultraviolet spectrum analysis was used to study the properties of gold nanoparticles. The maximum absorption of AuNPs was at 546 nm (Fig. 6), as the nanoparticles possess free electrons, and when subjected to a UV-visible source, the surface of the Plasmon is irritated. The electrons vibrate each other, which leads to an increase in the absorbance of the Plasmon [46]. Sharma *et al*. prepared the AuNPs by tea extract with different concentrations, so UV-visible 530-563 nm [26]. The absorbance peaks of AuNPs prepared using apple extract as a reducing agent were at 535-555nm [17, 47]. There is a strong relationship

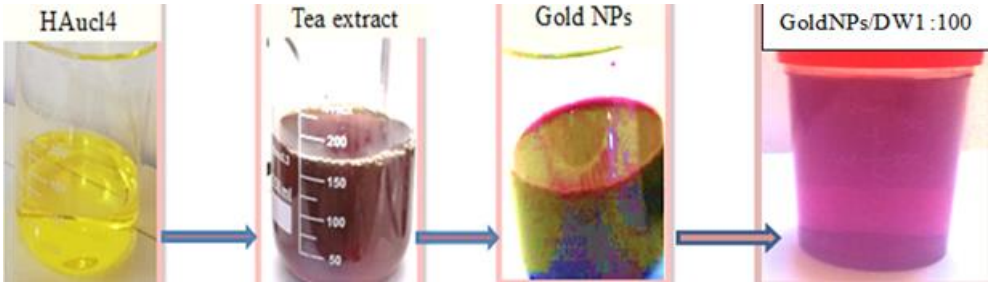

Fig. 5. Biosynthesis of gold nanoparticles using black tea extract as a reducing agent.

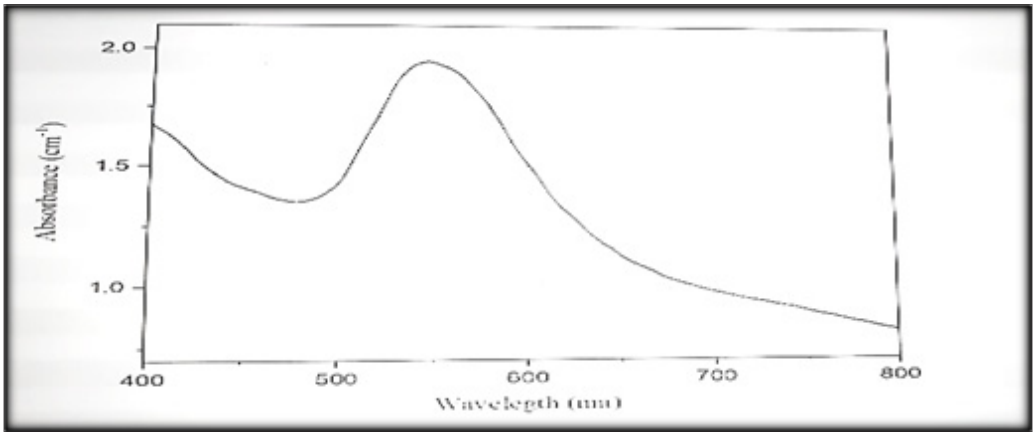

Fig. 6. UV-visible for AuNPs green synthesis by black tea extract

between the size of the AuNPs and the difference in the absorbance peaks, as the larger the NPs' size increases their absorption peaks [48].

Scanning Electron Microscopy (SEM) for the detection of gold nanoparticles

The gold nanoparticles deposited on the slide were examined using a scanning electron microscope (SEM), which was accurately prepared for the surface topography of the NPs. A scanning electron microscope (SEM) showed the shape and size of the AuNPs, which were spherical or semi-spherical in shape and size of 19.11 nm (Fig. 7).

These results showed a mismatch with Parida *et al*, as they found that the size of gold NPs manufactured by using onion extract as the reducing agent was about 100 nm with cubic and spherical shapes [49]. Nun et al, indicated that the size of the AuNPs was 15-45 nm and had a spherical shape after its preparation with tea extract as a reducing agent [43]. Also, it contradicted the results of Samanta *et al*. They synthesized AuNPs using the fungus *Laccaria fraterna* as a reducing agent. They found that the AuNPs size was 79.69 nm with different shapes [30]. The difference in the size of AuNPs is due to the difference in the

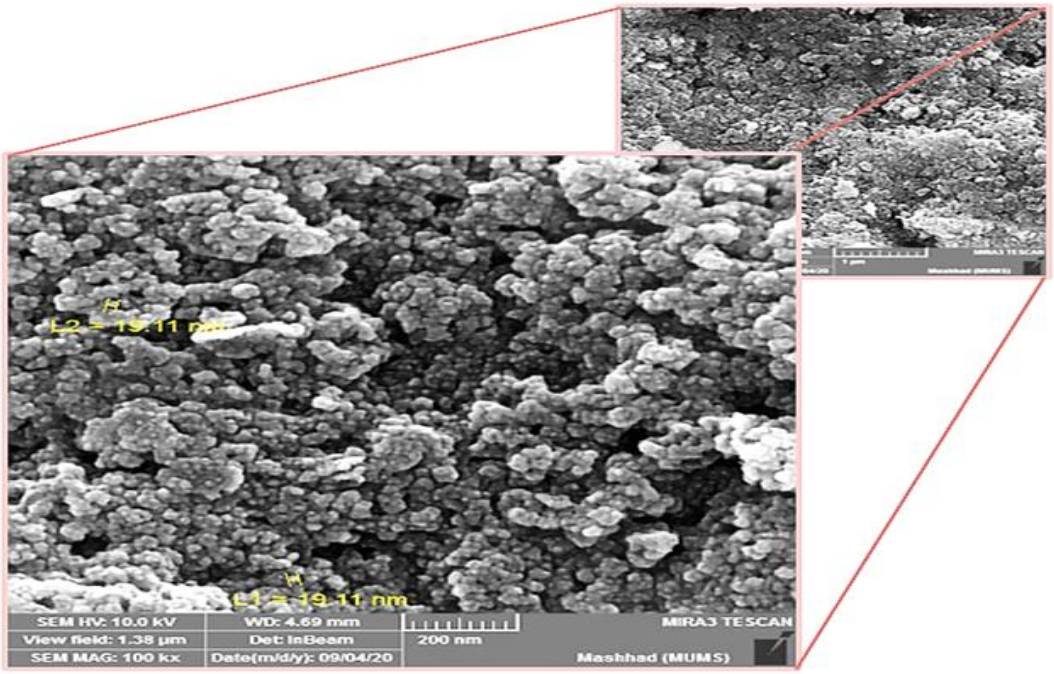

Fig. 7. Scanning Electron Microscopy (SEM) for green synthesized AuNPs with size (19.11 nm), spherical and collected in the cluster of 200 nm dimensions, the image is dimensioned (1.38x1.38 µm) and zoom ratio 200kx.

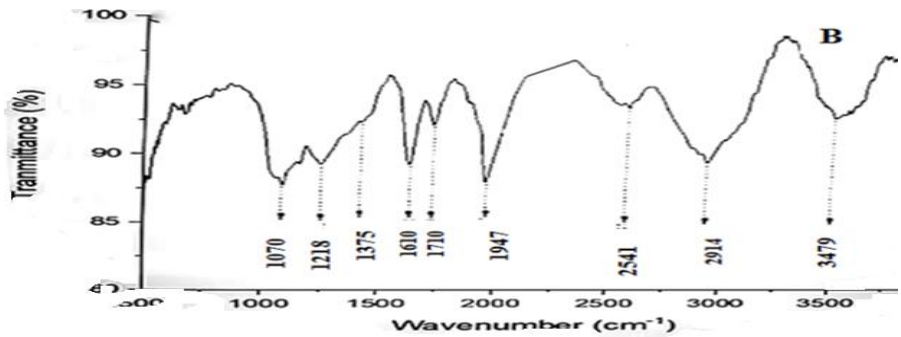

Fig. 8. IR-spectra analysis for green synthesized AuNPs.

type of extract used as an oxidizing agent for the gold chloride reduction, as well as the difference in the concentration of the extract [50].

FT-IR analysis of gold nanoparticles (AuNPs)

The infrared spectrum analysis was used to identify the functional groups responsible for the formation and stability of AuNPs. The analysis results are shown in (Fig. 8), which showed the presence of a strong peak at 3479 cm $^{-1}$, representing a bond in the O-H group of tea extract involved in the biosynthesis of AuNPs [51]. Also, the presence of a strong absorbance band at 2970 cm^{-1} indicated the C-H bond in alkane groups, an absorbance peak at 1947 cm^{-1} represented (C=C), a band of absorbance at 1710 cm^{-1} indicated C=O stretching in carbonyl group [16]. The band of absorbance at 1610 cm^{-1} for C=N stretching of the amide group in the proteins. The peak located at 2541cm^{-1} was attributed to the N–H stretching vibrations [52]. The absorbance peaks at 1070 cm^{-1} were for C- aliphatic amines, and the weak band was at 1375 cm^{-1} for C-N functional group in aromatic amines. The band at 1218 cm^{-1} for C-O stretching is related to polyphenols [53].

The presence of an absorbance peak at 3479 cm^{-1} showed the involvement of the -OH group of polyphenols as catechins in the green synthesis of AuNPs, and the band at 1392 cm^{-1} illustrates the presence of caffeine [54]. The absorbance peaks at 1070, 1610, and 1218 cm^{-1} demonstrate that AuNPs may bind to the protein through the carboxylate group [53]. These results follow previous reports [16, 17] and revealed the presence of black tea polyphenols as reducing agents in the biosynthesis of AuNPs, which gave stability to the NPS [43].

X-ray diffraction analysis (XRD) for the detection of gold NPs

X-ray diffraction analysis (XRD) was used to find the crystal structure of AuNPs fixed on a glass slide using an X-ray beam incident. The crystal

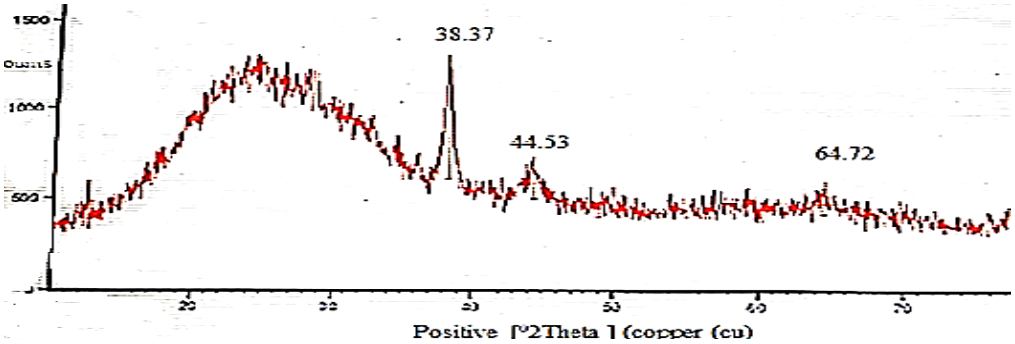

Fig. 9. X-ray Diffraction of gold NPs surface

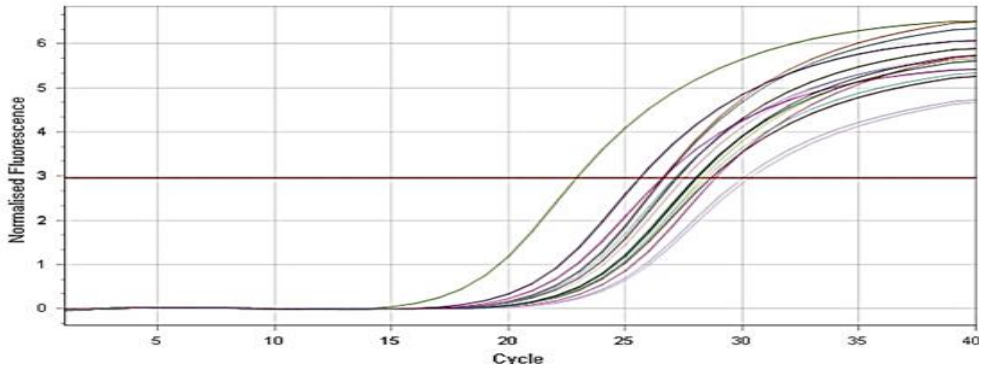

Fig. 10. Curves of cycle threshold (CT) values for gene expression of *hmgA* gene.

Table 1. Gene expression values for *hmgA* and reference genes.

Conc. (µg/ml)	*oprl* gene	*hmgA* gene	DCT	DDCT	Fold±S.E.
Stock con.	21.22	25.63	4.41	-0.74	1.68±0.95
320	20.84	22.91	2.08	-3.08	8.45 ±0.95
160	23.66	26.61	2.95	-2.21	4.62 ±0.95
80	22.27	26.67	4.40	-0.76	1.69 ±0.95
40	21.83	27.22	5.39	0.24	0.85 ±0.95
20	22.10	27.55	5.45	0.29	0.82 ±0.95
10	21.83	27.12	2.29	0.14	0.91 ±0.95
Control	21.45	26.61	5.15	0.00	1.00 ±0.95

structure of the AuNPs appeared with three peaks (Fig. 9), corresponding to the standard Prague diffraction or reflections 111, 200, and 220. The strong peak at 38.37 corresponds to 111, whereas peaks at 44.53° and 64.72° correspond to 200 and 220, respectively. These results agree with those reported by Mishra et al., who indicated that the XRD gold NPs had three peaks: 38.1, 44.56, and 64.74 [55]. Also, the results agree with Long *et al*., who demonstrated the three peaks corresponding to the standard X-ray diffractions 111, 200, and 220 [56].

Assessment of the effect of gold nanoparticles on pigment production

The effect of gold NPs on the pigment production genes was detected by using the real-time technique, by culturing isolates on broth media suitable for producing inoculated pigments with different concentrations of AuNPs (0, 10, 20, 40, 80, 160, 320, and 10000 µg/ml. RNA was extracted from these replicates in 10-500 ng/µl. The real-time one-step technique was used to quantify the gene expression level of *hmgA* genes compared to the *oprl* gene (reference gene).

The effect of gold- NPs on hmgA gene expression

Cycle Threshold (CT) is the basic rule for the amount of gene expression in qRT-PCR (Fig. 10), the cycle in which the maximum fluorescence in the curve expresses the amount of gene expression, measured by the one-step method. In which RNA is converted to cDNA in a single tube. Gene expression was measured by the relative method, in which the target sample's gene expression is estimated based on a reference sample known as control. The gene expression is quantified for each sample, and the CT results for each sample are compared with the CT results for gene expression of the reference gene. Gene expression values were computed according to the Livak method.

One sample t-test was used to compare the difference between means of gene expression in folding. The differences in the folding of the *hmgA* gene were significant (P< 0.03) (t=2.60, d. f=7). The treatment with gold NPs led to an increase in the gene expression of the *hmgA* gene at a concentration of 80 µg / ml to 1.69-fold in comparison to the control; also, the gene expression was 4.62-fold at 160 µg/ml concentration, 8.45, and 1.68-fold at 320 and 10000 µg / ml concentration, respectively (Table 1) [57].

The gold NPs did not show toxicity to *P. aeruginosa* but could affect cellular communication systems, which affects the expression of some virulence factors [18]. The nanoparticles were used directly in a study of AgNPs that caused a decrease in the gene expression fold value of the PKS1and SCD1 genes responsible for the production of the melanin pigment in Bipolaris sorokiniana fungus at concentrations of 0.1, 0.05 mg/ml [58]. Nanoparticles (NPs) have several features, including a large surface area, the ability to penetrate cells and reach within a size of less than a micron with fast absorption ability [60, 61, 63], so they have been used to transport nucleic acids that can alter or change cellular gene expression it is also considered distinguished as an excellent means of altering cellular gene expression [14, 59, 62]. The increased gene expression can be attributed to the production of pigments in *P. aeruginosa* to resist the effect of nanoparticles, a possible additional resistance mechanism in clinical isolates of *P. aeruginosa* [59].

CONCLUSION

This study showed a significant effect of gold nanoparticles on the *hmgA* gene expression. Specific concentrations of gold NPs have induced the expression of the *hmgA* gene, which is involved in the production of pigments to resist the effect

of the nanoparticles, which leads to increasing the production of coloring as a means of resistance. These gold NPs did not have a toxic consequence on *P. aeruginosa.*

CONFLICT OF INTEREST

The authors declare that there is no conflict of interests regarding the publication of this manuscript.

REFERENCES

1. Hardalo C, Edberg SC. Pseudomonas aeruginosa: Assessment of Risk from Drinking Water. Crit Rev Microbiol. 1997;23(1):47-75.
2. Bodey GP, Bolivar R, Fainstein V, Jadeja L. Infections Caused by Pseudomonas aeruginosa. Clin Infect Dis. 1983;5(2):279-313.
3. Shaebth L. Molecular identification and sequencing of Pseudomonas aeruginosa virulence genes among different isolates in Al-Diwaneyah hospital. Iraqi Journal of Veterinary Sciences. 2019;32(2):183-188.
4. Chemical Inhibition of Kynureninase Reduces Pseudomonas aeruginosa Quorum Sensing and Virulence Factor Expression. American Chemical Society (ACS).
5. Lau GW, Hassett DJ, Ran H, Kong F. The role of pyocyanin in Pseudomonas aeruginosa infection. Trends Mol Med. 2004;10(12):599-606.
6. Baron SS, Rowe JJ. Antibiotic action of pyocyanin. Antimicrobial agents and chemotherapy. 1981;20(6):814-820.
7. Bilen Özyürek S, Diken Gü Sr, Seyis Bilkay I. Investigation of Antimicrobial Activity of Pyocyanin Produced by Pseudomonas aeruginosa Strains Isolated from Different Clinical Specimens. Hacettepe Journal of Biology and Chemistry. 2016;1(44):1-1.
8. Hunter RC, Newman DK. A putative ABC transporter, hatABCDE, is among molecular determinants of pyomelanin production in Pseudomonas aeruginosa. J Bacteriol. 2010;192(22):5962-5971.
9. Wang Z, Lin B, Mostaghim A, Rubin RA, Glaser ER, Mittraparp-Arthorn P, et al. Vibrio campbellii hmgA-mediated pyomelanization impairs quorum sensing, virulence, and cellular fitness. Front Microbiol. 2013;4:379-379.
10. Higby GJ. Gold in medicine. Gold Bulletin. 1982;15(4):130-140.
11. Richards DG, McMillin DL, Mein EA, Nelson CD. Gold and its relationship to neurological/glandular conditions. Int J Neurosci. 2002;112(1):31-53.
12. Skrabalak SE, Chen J, Au L, Lu X, Li X, Xia Y. Gold Nanocages for Biomedical Applications. Advanced materials (Deerfield Beach, Fla). 2007;19(20):3177-3184.
13. Thakur S, Saini RV, Singh P, Raizada P, Thakur VK, Saini AK. Nanoparticles as an emerging tool to alter the gene expression: Preparation and conjugation methods. Materials Today Chemistry. 2020;17:100295.
14. Panyam J, Zhou WZ, Prabha S, Sahoo SK, Labhasetwar V. Rapid endo-lysosomal escape of poly(DL-lactide-co-glycolide) nanoparticles: implications for drug and gene delivery. The FASEB Journal. 2002;16(10):1217-1226.
15. D.G. San Diego K, Ian A. Alindayu J, Q. Baculi R. Biosynthesis of gold nanoparticles by bacteria from hyperalkaline spring and evaluation of their inhibitory activity against pyocyanin production. Journal of microbiology, biotechnology and food sciences. 2018;8(2):781-787.
16. Yu Q, Li J, Zhang Y, Wang Y, Liu L, Li M. Inhibition of gold nanoparticles (AuNPs) on pathogenic biofilm formation and invasion to host cells. Sci Rep. 2016;6:26667-26667.
17. García-Lara B, Saucedo-Mora MÁ, Roldán-Sánchez JA, Pérez-Eretza B, Ramasamy M, Lee J, et al. Inhibition of quorum-sensing-dependent virulence factors and biofilm formation of clinical and environmental Pseudomonas aeruginosa strains by ZnO nanoparticles. Lett Appl Microbiol. 2015;61(3):299-305.
18. Saleh BH. Study of cytotoxicity of purified toxin A produced from pseudomonas aeruginosa on cell lines. Iraqi Journal of Cancer and Medical Genetics. 2018;6(2).
19. Mahmood, et al. Relationship between pigments production and biofilm formation from local pseudomonas aeruginosa isolates. iraqi journal of agricultural sciences. 2020;51(5):1413-1419.
20. Singh D, Kumar J, Kumar A. Isolation of pyomelanin from bacteria and evidences showing its synthesis by 4-hydroxyphenylpyruvate dioxygenase enzyme encoded by hppD gene. Int J Biol Macromol. 2018;119:864-873.
21. Al-Daraghi WA. Detection of Exotoxin A gene in Pseudomonas aeruginosa from Clinical and Environmental samples. Journal of Al-Nahrain University Science. 2013;16(2):167-172.
22. Yuan W, Burleigh SH, Dawson JO. Melanin biosynthesis by Frankia strain CeI5. Physiol Plant. 2007;131(2):180-190.
23. Gatea DIH. Bioplastic (poly -3-hydroxybutyrate) production by local pseudomonas aeruginosa isolates utilizing waste cooking oil. World Journal of Pharmaceutical Research. 2017:289-302.
24. Ellis DH, Griffiths DA. The location and analysis of melanins in the cell walls of some soil fungi. Can J Microbiol. 1974;20(10):1379-1386.
25. Sharma RK, Gulati S, Mehta S. Preparation of Gold Nanoparticles Using Tea: A Green Chemistry Experiment. J Chem Educ. 2012;89(10):1316-1318.
26. Behnia B, Safardoust-Hojaghan H, Amiri O, Salavati-Niasari M, Anvari AA. High-performance cement mortars-based composites with colloidal nano-silica: Synthesis, characterization and mechanical properties. Arab J Chem. 2021;14(9):103338.
27. Saliem AH, Ibrahim OMS, Salih SI. Biosynthesis of Silver Nanoparticles using Cinnamon zeylanicum Plants Bark Extract. Kufa Journal For Veterinary Medical Sciences. 2016;7(1):51-63.
28. Thaira H, Raval R, Raval K. Adsorptive Bioprocess Improves Yield of Melanin from Pseudomonas stutzeri. Journal of Visualized Experiments. 2022(179).
29. Samanta S, Singh BR, Adholeya A. Intracellular Synthesis of Gold Nanoparticles Using an Ectomycorrhizal Strain EM-1083 of Laccaria fraterna and Its Nanoanti-quorum Sensing Potential Against Pseudomonas aeruginosa. Indian J Microbiol. 2017;57(4):448-460.
30. Greene JJ. Isolation and Purification of Nucleic Acids. Recombinant DNA Principles and Methodologies: CRC Press; 2021. p. 271-302.
31. Daniel M-C, Astruc D. Gold Nanoparticles: Assembly, Supramolecular Chemistry, Quantum-Size-Related Properties, and Applications toward Biology, Catalysis, and Nanotechnology. Chem Rev. 2003;104(1):293-346.
32. Salmen SH. Biosynthesis of Silver Nanoparticles from Date (Phoenix dactylifera) Seeds Extract and Evaluation of

Antibacterial Activity Against Pathogenic Bacteria. Oriental Journal Of Chemistry. 2020;36(6):1189-1193.
33. Rodríguez-Rojas A, Mena A, Martín S, Borrell N, Oliver A, Blázquez J. Inactivation of the hmgA gene of Pseudomonas aeruginosa leads to pyomelanin hyperproduction, stress resistance and increased persistence in chronic lung infection. Microbiology. 2009;155(4):1050-1057.
34. Schmaler-Ripcke J, Sugareva V, Gebhardt P, Winkler R, Kniemeyer O, Heinekamp T, et al. Production of pyomelanin, a second type of melanin, via the tyrosine degradation pathway in Aspergillus fumigatus. Applied and environmental microbiology. 2009;75(2):493-503.
35. Sajjan SS. Properties and Functions of Melanin Pigment from Klebsiella sp. GSK. Korean Journal of Microbiology and Biotechnology. 2013;41(1):60-69.
36. Turick CE, Knox AS, Becnel JM, Ekechukwu AA, Millike CE. Properties and Function of Pyomelanin. Biopolymers: Sciyo; 2010.
37. Schaeffer P. A black mutant of Neurospora crassa. mode of action of the mutant allele and action of light on melanogenesis. Archives of Biochemistry and Biophysics. 1953;47(2):359-379.
38. Sansinenea E, Ortiz A. Melanin: a photoprotection for Bacillus thuringiensis based biopesticides. Biotechnology Letters. 2014;37(3):483-490.
39. Brenner M, Hearing VJ. The protective role of melanin against UV damage in human skin. Photochemistry and photobiology. 2008;84(3):539-549.
40. Bilińska B. Progress of infrared investigations of melanin structures. Spectrochimica Acta Part A: Molecular and Biomolecular Spectroscopy. 1996;52(9):1157-1162.
41. David C, Daro A, Szalai E, Atarhouch T, Mergeay M. Formation of polymeric pigments in the presence of bacteria and comparison with chemical oxidative coupling—II. Catabolism of tyrosine and hydroxyphenylacetic acid by Alcaligenes eutrophus CH34 and mutants. Eur Polym J. 1996;32(6):669-679.
42. Behnia B, Anvari AA, Safardoust-Hojaghan H, Salavati-Niasari M. Positive effects of novel nano-zirconia on flexural and compressive strength of Portland cement paste. Polyhedron. 2020;177:114317.
43. Hamdan AB, Suryanto, Haider FI. Study on tea leaves extract as green corrosion inhibitor of mild steel in hydrochloric acid solution. IOP Conference Series: Materials Science and Engineering. 2018;290:012086.
44. Noginov MA, Zhu G, Bahoura M, Adegoke J, Small C, Ritzo BA, et al. The effect of gain and absorption on surface plasmons in metal nanoparticles. Appl Phys B. 2006;86(3):455-460.
45. Dorjnamjin D, Ariunaa M, Shim YK. Synthesis of silver nanoparticles using hydroxyl functionalized ionic liquids and their antimicrobial activity. Int J Mol Sci. 2008;9(5):807-820.
46. Yudono B, Rahmat A, Said M, Ningsi AI. Effect of Salinity Levels on Petroleum Recovery Using Bio Surfactant of Pseudomonas Peli Bacteria and Pseudomonas Flourescens. Elsevier BV; 2023.
47. Husseiny MI, El-Aziz MA, Badr Y, Mahmoud MA. Biosynthesis of gold nanoparticles using Pseudomonas aeruginosa. Spectrochimica Acta Part A: Molecular and Biomolecular Spectroscopy. 2007;67(3-4):1003-1006.
48. Parida UK, Bindhani BK, Nayak P. Green Synthesis and Characterization of Gold Nanoparticles Using Onion (Allium cepa) Extract. World Journal of Nano Science and Engineering. 2011;01(04):93-98.
49. J. Haider A, A. Shabeeb D, Th. Mohammed A. Synthesis and stabilization of gold nanoparticles by inverse reduction method using sodium citrate and sodium boro hydride as reducing agent. Journal of University of Anbar for Pure Science. 2016;10(1):37-47.
50. Lee YJ, Ahn E-Y, Park Y. Shape-dependent cytotoxicity and cellular uptake of gold nanoparticles synthesized using green tea extract. Nanoscale research letters. 2019;14(1):129-129.
51. Bankar A, Joshi B, Ravi Kumar A, Zinjarde S. Banana peel extract mediated synthesis of gold nanoparticles. Colloids Surf B Biointerfaces. 2010;80(1):45-50.
52. Aswathy Aromal S, Philip D. Green synthesis of gold nanoparticles using Trigonella foenum-graecum and its size-dependent catalytic activity. Spectrochimica Acta Part A: Molecular and Biomolecular Spectroscopy. 2012;97:1-5.
53. Mohammad-Salehi H, Hamadanian M, Safardoust-Hojaghan H. Visible-light induced Photodegradation of methyl Orange via palladium nanoparticles anchored to chrome and nitrogen doped TiO_2 nanoparticles. Journal of Inorganic and Organometallic Polymers and Materials. 2019;29:1457-1465.
54. Mishra A, Harper S, Yun S-I. Interaction of biosynthesized gold nanoparticles with genomic DNA isolated from E. coli and S. aureus. 2011 11th IEEE International Conference on Nanotechnology; 2011/08: IEEE; 2011. p. 1745-1750.
55. Long NN, Vu LV, Kiem CD, Doanh SC, Nguyet CT, Hang PT, et al. Synthesis and optical properties of colloidal gold nanoparticles. Journal of Physics: Conference Series. 2009;187:012026.
56. Production of antimicrobial blue green pigment Pyocyanin by marine Pseudomonas aeruginosa. Biointerface Research in Applied Chemistry. 2019;9(5):4334-4339.
57. Mishra S, Singh HB. Silver nanoparticles mediated altered gene expression of melanin biosynthesis genes in Bipolaris sorokiniana. Microbiol Res. 2015;172:16-18.
58. Gómez-Zorrilla S, Camoez M, Tubau F, Periche E, Cañizares R, Dominguez MA, et al. Antibiotic pressure is a major risk factor for rectal colonization by multidrug-resistant Pseudomonas aeruginosa in critically ill patients. Antimicrobial agents and chemotherapy. 2014;58(10):5863-5870.
59. Nasir GA, Khudhair IA, Najm MA, Mahmood HM. Nanotechnology at the Molecular Level. Al-Rafidain Journal of Medical Sciences (ISSN: 2789-3219). 2022;3:71-74.
60. Tiba AA-M, Huda MM. Carbapenem Resistance Related with Biofilm Formation and Pilin Genes in Clinical Pseudomonas aeruginosa Isolates. Iraqi Journal of Pharmaceutical Sciences(P-ISSN 1683 - 3597 E-ISSN 2521 - 3512). 2024;33(1):72-78.
61. Mobinhosseini F, Salehirad M, Wallace Hayes A, Motaghinejad M, Hekmati M, Safari S, et al. Curcumin-ZnO conjugated nanoparticles confer neuroprotection against ketamine-induced neurotoxicity. Journal of Biochemical and Molecular Toxicology. 2023;38(1).
62. Fratoddi I, Venditti I, Cametti C, Russo MV. Gold nanoparticles and gold nanoparticle-conjugates for delivery of therapeutic molecules. Progress and challenges. J Mater Chem B. 2014;2(27):4204-4220.
63. Wang CC, Wu SM, Li HW, Chang HT. Biomedical Applications of DNA-Conjugated Gold Nanoparticles. ChemBioChem. 2016;17(12):1052-1062.